

Coarse-grained simulations of solute diffusion in crosslinked flexible hydrogels.

Manuel Quesada-Pérez^{1*}, José-Alberto Maroto-Centeno¹, María del Mar Ramos-Tejada¹ and Alberto Martín-Molina^{2,3}

¹Departamento de Física, Escuela Politécnica Superior de Linares, Universidad de Jaén, 23700, Linares, Jaén, Spain.

Emails: mquesada@ujaen.es , jamaroto@ujaen.es , mmramos@ujaen.es

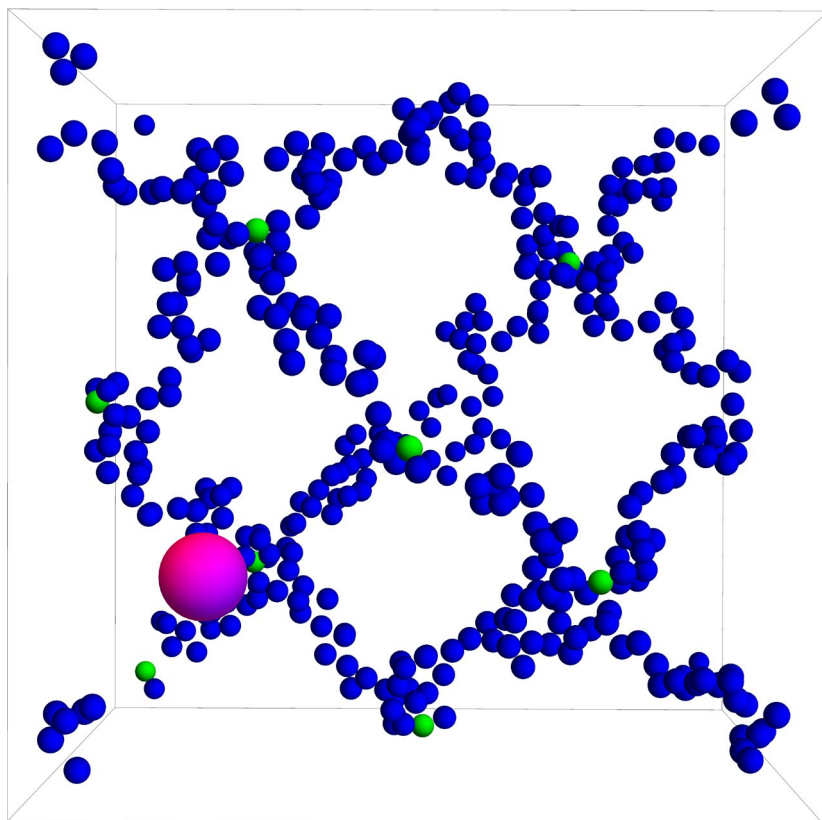
²Departamento de Física Aplicada, Universidad de Granada, Campus de Fuentenueva s/n, 18071 Granada, Spain.

Email: almartin@ugr.es

³Instituto Carlos I de Física Teórica y Computacional, Universidad de Granada, Campus de Fuentenueva s/n, 18071 Granada, Spain

(*) Corresponding author

TABLE OF CONTENTS



Coarse-grained model employed to compute diffusion coefficients.

ABSTRACT.

In this work, the long-time diffusion of a solute in a chemically crosslinked and flexible hydrogel is computed from a coarse-grained model of polymeric network. The effects of different key parameters of this model on diffusion are assessed. The relevance of chain flexibility becomes important with increasing the polymer volume fraction and the solute size. In fact, the solute particle can moderately diffuse in flexible hydrogels even when its diameter is comparable to the mesh size. The diffusion coefficients obtained here are tested comparing with previously reported experimental data. A reasonably good agreement between experiment and simulation is found without requiring any adjustable parameter.

INTRODUCTION.

The diffusion of macromolecules and nanoparticles particles through crosslinked gels is of fundamental importance in many technological processes, such as size exclusion chromatography and drug delivery. Solute diffusion also plays a key role in biopolymer-based protective hydrogels, such as mucus. However, the physical mechanisms that explain why only some particles can permeate such barriers are not fully understood yet. In any case, knowing the relationship between the solute diffusivity and the parameters describing the polymer network, such as the polymer volume fraction (φ) or the mesh size (ξ), can become a powerful tool for the design and development of functional gels and for the understanding of hydrogels of biological interest.

For these reasons, many theorists have developed expressions to predict diffusion coefficients from structural parameters of the polymer network (and the solute radius). Amsden¹ and Masaro *et al.*² reviewed these models at the late nineties. Some of these theories are based on the concept of free volume, which is defined as the volume not occupied by molecules of the solvent or the polymer. The rearrangement of the free volume produces voids through which solute particles are able to diffuse. Other models are based on the concept of obstruction. Polymer chains are considered as fixed and impenetrable obstacles that slow down the diffusive motion of the solute. But, according to hydrodynamic theories, polymeric chains slow down the fluid near them, which increases the friction drag on the solute and reduces its diffusion coefficient. Recently, Axpe *et al.* have combined a free volume model and an obstruction model, which are supposed to operate at different length scales.³

Although the expressions derived from all these theories might be quite appealing for experimentalists, we should keep in mind that such theories suffer from some limitations. In fact, Amsden and Masaro *et al.* concluded that many of their characteristic parameters are not known a priori, which significantly reduces its capability of prediction.^{1,2} In our

opinion, we should also stress that these theories usually neglects the flexibility of the polymeric chains, which are considered fixed centers of hydrodynamic resistance.

Computer simulations can be a useful tool to address different issues related to diffusion in gels.⁴⁻⁸ In fact, many researchers have simulated diffusive processes in gel-like systems since the early nineties. Most of them modelled gels as rigid structures of different geometry, such as wormlike chains made of spherical beads,⁹⁻¹¹ self-avoiding random walks,^{12,13} randomly distributed points or obstacles,^{13,14} points along the sides of cubes,¹⁴ beads along the sides and the nodes of a cubic lattice,^{15,16} parallel rods,^{11,17} straight fibers with different orientations¹⁸ and infinite rods in the three spatial directions.¹⁹⁻²² The existence of crosslinks between polymeric chains was explicitly considered by Netz *et al.*,¹² Miyata *et al.*,^{15,16} and Hansing *et al.*^{19,20,22}

Some flexible gel-like structures have also been simulated. Licinio, Zhou, Sandrin and their respective coworkers connected spheres initially placed at the nodes of a cubic lattice through harmonic potentials.²³⁻²⁵ It should be noted, however, that their simulations did not explicitly consider polymeric chains. Similarly, Kumar *et al.* created a polymer network on a diamond lattice consisting of 9883 monomers²⁶ in which each monomer was connected to four neighboring monomers through a finitely extensive nonlinear elastic (FENE) spring characterized by a constant k , a measure of the network stiffness. In addition, Kumar *et al.* also looked into the effect of stickiness between the solute and the polymer network.²⁶ Likewise, Godec *et al.* considered a gel of $7 \times 7 \times 7$ connected beads with a simple unit cell and a freely diffusing tracer bead.²⁷ Nearest neighbors were connected via Morse springs, and the authors used two different values for the depth of the Morse potential that represent a moderately soft and a rather stiff gel. Kumar, Godec and their respective coworkers concluded that the flexibility of the gel-like structure plays a key role when the diameter of the tracer is similar to the mesh size or larger.

The bead-spring model of polymeric network has also been used to simulate solute diffusion in gels. This coarse-grained model, employed to study gel swelling and solute partitioning from the early 2000s²⁸⁻³⁵, allows us to explicitly consider crosslinked flexible polymer chains.^{4,36,37} The model is particularly appropriate to explicitly consider solute-monomer and solute-crosslinker interactions or to simulate tightly-meshed networks.^{35,37-39} In addition, polydispersity or entanglements can also be implemented.^{40,41}

Recently, we have simulated an assortment of crosslinked flexible hydrogels finding that their relative diffusivity admits a single and unified description in terms of a new parameter β , defined as $\beta = \varphi(1 + R_s/R_p)^{1.3}$,⁴² where R_s and R_p are the radius of the solute and the radius of the polymeric chains or fibers that constitute the gel, respectively. Here we extend our previous work on flexible crosslinked gels performing a systematic study on the effect of certain aspects of the bead-spring model (such as chain flexibility, particle stiffness or degree of crosslinking) on solute diffusion. Special attention is paid to the effect of mesh size. This parameter plays an important role in some models of solute diffusion in gels although its experimental determination is ambiguous.⁴³ Luckily, simulations can yield accurate values of this parameter. Our simulation data are also compared to results obtained for rigid gels. In this way, the effect of chain flexibility can be more clearly evaluated. In addition, we find out to what extent the bead-spring model used here can reproduce experimental diffusion coefficients. The direct comparison between the predictions of simulations and real data allows us to assess the reliability of the model and its approximations in applications to real situations. More specifically, we test the model comparing with recent measurements of the diffusion coefficient in poly(ethylene glycol) diacrylate (PEGDA) hydrogels.^{44,45} Poly(ethylene glycol)-based hydrogels are used in a variety of biomedical applications (including drug delivery and

regenerative medicine because they do not generally elicit an immune response)⁴⁶ and can be covalently crosslinked with the help of reactive chain ends, such as acrylate.

MODEL AND SIMULATIONS.

According to the bead-spring model of crosslinked gel, the solvent is a continuous medium and each monomeric unit forming the polymer chain is modeled as a sphere of radius R_m . The radius of monomeric units must be quite similar to the radius of the molecule of the corresponding monomer. In turn, this radius can be estimated from the density (ρ_m) of the monomer (in the liquid state) and the molecular weight (M_m) as $R_m \approx \sqrt[3]{0.74 \cdot 3M_m/4\pi N_A \rho_m}$, where N_A is Avogadro's number. The radius of many monomers, such as vinyl acetate, *N*-vinyl-2-pyrrolidone, *N*-isopropyl acrylamide and ethylene glycol, is close to 0.3 nm. Consequently, this value was used for the monomeric units and the crosslinkers in the simulations carried out here. The solute particle is also modeled as a sphere whose radius is R_s . In this work, this parameter ranges from 0.6 to 2.2 nm (in round numbers). This range includes many typical drugs and small macromolecules.

The steric forces between any pair of particles (solute, monomeric units or crosslinkers) due to excluded volume effects were included in the model through the Weeks-Chandler-Andersen (WCA) potential:

$$u_{WCA}(r) = \begin{cases} \varepsilon_{WCA}((d/r)^{12} + (d/r)^6 + 1/4) & r \leq \sqrt[6]{2}d \\ 0 & r > \sqrt[6]{2}d \end{cases} \quad (1)$$

Here r is the center-to-center distance between a given pair of particles, ε_{WCA} is the parameter describing the strength of this interaction and $d = R_i + R_j$ (where R_i stands for the radius of species i). In our previous works, $\varepsilon_{WCA} = 4.11 \cdot 10^{-21}$ J, which is equivalent to $k_B T$ (where k_B is Boltzmann's constant and T the absolute temperature) for $T = 298$ K. This will also be the value used in these simulations unless otherwise stated.

We should bear in mind that, unlike the Lennard-Jones potential, the WCA potential is purely repulsive and ε_{WCA} is related to the rigidity of the interacting particles.

Four polymer chains are connected to each crosslinker following a diamond-like topology (see Figure 1).

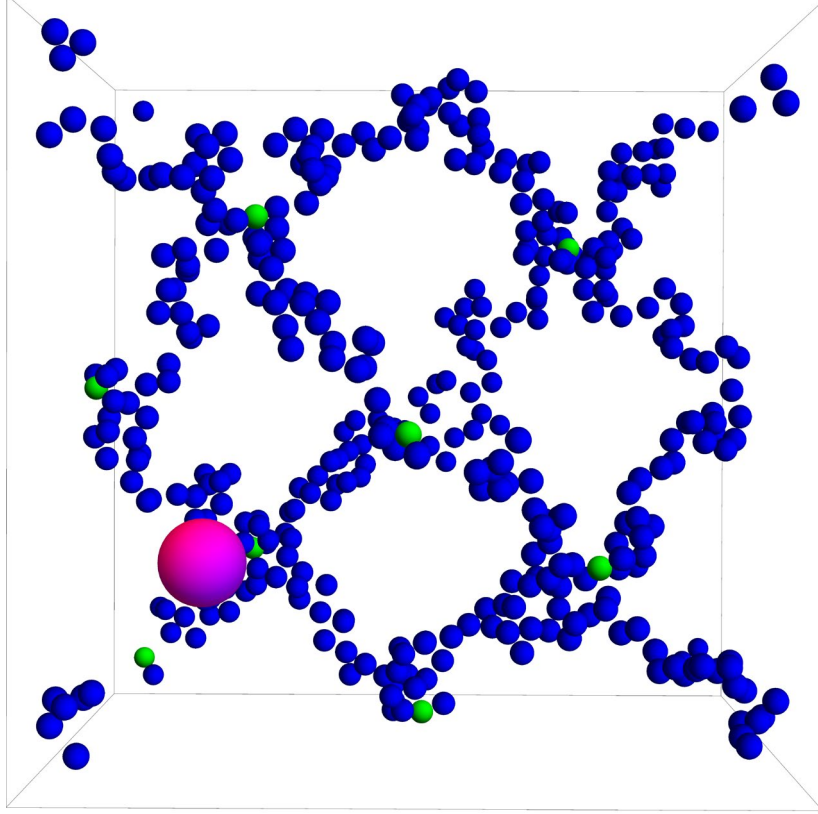


Figure 1. Snapshot of the simulation cell corresponding to a gel of 25 monomeric units per chain and a solute particle whose radius is 1 nm. Blue, green and magenta beads represent monomeric units, crosslinkers and solute particle, respectively.

For ideal networks, it is usually assumed that each polymer chain contains the same number of monomeric units (N_{mu}). The forces between bonded monomeric units can be derived from a harmonic potential:

$$u_e(r) = 0.5k_e(r - r_0)^2 \quad (2)$$

In this expression, k_e is the elastic constant of the bonds between neighboring monomeric units and r_0 is the equilibrium distance ($r_0 = 2R_m$ was assumed). According to some authors,²⁹ k_e must be greater than $k_B T / (2R_m)^2$. In this way, the thermal fluctuations

undergone by monomeric units are smaller than their diameter and the polymeric network is stable. The k_e -values used in this work satisfied this criterion.

Given that simulating the whole gel is not feasible, our simulations are restricted to a cubic unit cell containing 16 chains connected by 8 crosslinkers and the solute particle.

Periodic boundary conditions are applied to replicate the unit cell in the three spatial directions. Simulations were performed in the canonical ensemble (constant volume, temperature and number of particles). The total number of particles in the simulation box depends on the number of monomeric units per chain. The dimensions of the simulation cell were adjusted in every simulation to reproduce the polymer volume fraction desired.

The conventional Brownian Dynamics (BD) algorithm was used to move the particles of the unit cell. If hydrodynamic interactions are not present, the m -component (where m stands for the Cartesian spatial directions x , y or z) of the displacement of particle i during a time step Δt can be computed as:⁴⁷

$$\Delta r_{m,i} = \sqrt{2D_{0,i}\Delta t}N(0,1) + F_{m,i}\Delta t/k_B T \quad (3)$$

where $D_{0,i}$ is the free diffusion coefficient of the particle in the solvent, $N(0,1)$, is a random number generated according to a Gaussian distribution of zero mean and unit standard deviation and $F_{m,i}$ is the m -component of the force exerted on particle i . This force can be derived from potentials (1) and (2). The free diffusion coefficient of a given particle was obtained from the Einstein-Stokes relationship, $D_{0,i} = k_B T / 6\pi\eta R_i$ (where η is the solvent viscosity). The Δt -value used in our simulations was 0.15 ps, which is of the order of that employed by other authors.¹¹ If Δt is not small enough, extremely large displacements and instabilities might occur during simulations.

The mean squared displacement (MSD) of the solute particle was computed averaging on 300 independent trajectories. The position of this particle was sampled every 30 ps for 30 ns for flexible gels and 60 ns for rigid gels. Consequently, $2 \cdot 10^5$ and $4 \cdot 10^5$ moves per

particle were executed, respectively, in every trajectory. Before collecting data for the computation of the MSD, $1 \cdot 10^5$ moves per particle were executed to equilibrate the polymer network. Several examples of MSD are provided as Supporting Information.

In a normal diffusive motion, the MSD ($\langle \Delta r^2 \rangle$) is proportional to time:

$$\langle \Delta r^2 \rangle = 6Dt \quad (4)$$

Here D stands for the self-diffusion coefficient. However, it should be stressed that, at very short times, the solute particle still does not “feel” the presence of the network. In other words, some time is required before the polymeric network fully affects the diffusive motion of the particle. The longtime diffusion coefficient was computed assuming that $\langle \Delta r^2 \rangle / 6t$ decays exponentially to D .⁴² The error bars of a few diffusion coefficients were estimated as the standard deviation of three independent runs to give an idea of their uncertainty.

RESULTS AND DISCUSSION

Effect of chain flexibility.

As mentioned in the introduction, this work focuses on gels made of crosslinked flexible polymeric chains, since they have been scarcely simulated so far. To begin with, let us analyze the effect of the chain flexibility itself. Figure 2 shows the relative diffusivity (D/D_0 , where D and D_0 stand for the longtime diffusion coefficient of the solute inside the gel and its free diffusion coefficient, respectively) as a function of the polymer volume fraction (φ) of a hydrogel with $N_{mu} = 25$ at 20 °C ($\eta = 0.0010$ Pa·s) and a solute particle with $R_s = 1$ nm. Four gels with different elastic constants have been simulated (0.04, 0.40, 1.0 and 4.0 N/m). In all cases, $k_e > k_B T / (2R_m)^2$. The error bars of a few data were computed from three independent runs to exemplify how large their uncertainty can be. The figure also includes the relative diffusivity obtained for rigid gels.

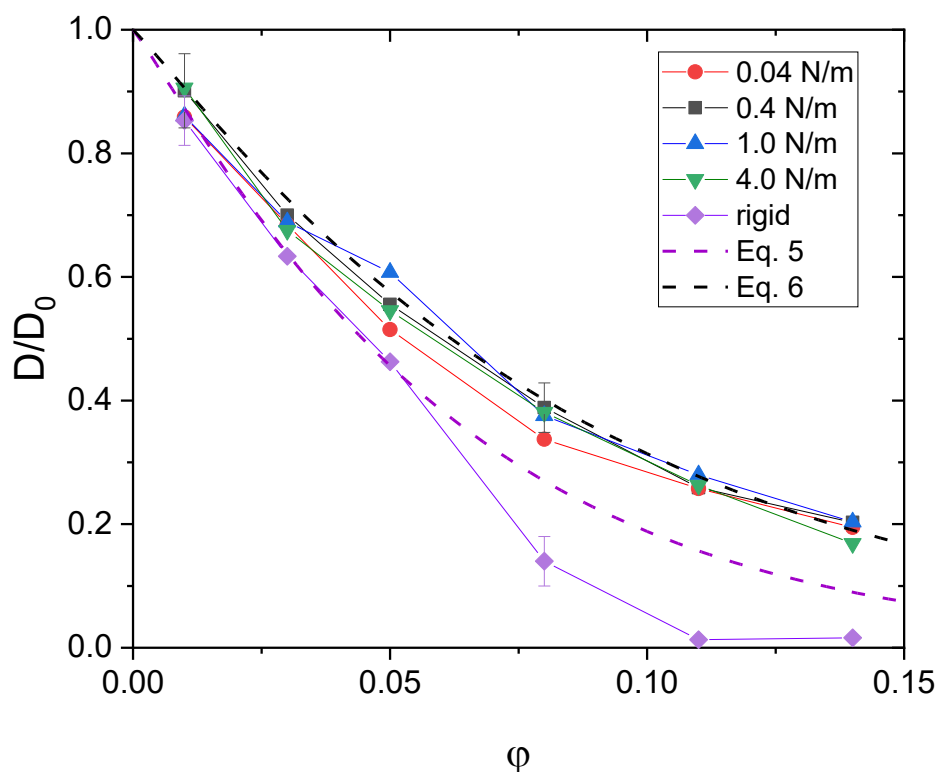


Figure 2. Relative diffusivity as a function of the polymer volume fraction for hydrogels with $N_{mu} = 25$ at 293 K and different elastic constants: $k_e = 0.04$ (circles), 0.40 (squares), 1.0 (up triangles) and 4.0 (down triangles) N/m. The solute radius is 1.0 nm. The results for a rigid hydrogel (diamonds) and the prediction proposed by Johansson *et al.*¹⁰, Equation 5 (dashed magenta line) and Quesada-Pérez *et al.*⁴², Equation 6 (dashed black line), are also plotted for comparison.

It can be concluded that: i) no significant differences are found when the elastic constant varies from 0.04 to 4.0 N/m; ii) at low polymer volume fractions, the effect of flexibility is negligible, since simulation results for flexible and rigid gels are almost identical. However, the differences between rigid and flexible gels become noticeable for $\phi \geq 0.08$. In fact, the diffusivity is very close to 0 for the rigid gel at $\phi \geq 0.11$. This means that the solute particle remains trapped inside the polymer backbone. On the contrary, the solute can moderately diffuse at these volume fractions if the gel is flexible.

Figure 2 also displays the prediction of D/D_0 proposed by Johansson and Löfroth for rigid gels:¹⁰

$$D/D_0 = \exp(-0.84\alpha^{1.09}) \quad (5)$$

Here $\alpha = \varphi(1 + R_s/R_p)^2$ where R_p is the polymer radius, which can be assumed to be close to radius of the monomeric units in the case of polymeric chains. It should be mentioned that Equation 5 was obtained fitting data with $\varphi \leq 0.05$ and $R_s \leq 3.0$ nm. According to Johansson and Löfroth, care should be taken when extrapolating beyond the ranges simulated. In fact, the diffusivities obtained here agree with Equation 5 only for $\varphi \leq 0.05$.

As mentioned previously, the diffusivity of an assortment of crosslinked flexible gels has been described with the help of a new parameter, $\beta = \varphi(1 + R_s/R_p)^{1.3}$,⁴²:

$$D/D_0 = \exp(-1.77\beta^{1.07}) \quad (6)$$

Although Equation 6 was derived for gels with $k_e = 0.40$ N/m, Figure 2 reveals that it also works reasonably well for k_e -values that vary by two orders of magnitude.

To probe the diffusive motion a little deeper, the Gaussian character of several representative cases of Figure 2 was analyzed computing the non-Gaussian parameter (α_2). For flexible gels, α_2 deviates from zero only slightly (see Supporting Information), which means that diffusion is Gaussian in a high degree. However, larger deviations can be found for rigid gels. This agrees with the results previously reported by Samanta *et al.* for gel-like structures.³⁹

It is worth investigating what happens for larger solute sizes. Figure 3 displays the relative diffusivity obtained in the same flexible gels at $\varphi = 0.08$ as a function of the solute radius. As can be seen, the diffusion coefficient decreases as the solute radius increases. Equation 6 is also able to predict this dependence with the size of the solute. It should be also stressed that, according to this equation, the relative diffusivity decreases with the solute radius more slowly for flexible gels, since β scales with $(1 + R_s/R_p)^{1.3}$ whereas α (the parameter characterizing rigid gels) scales with $(1 + R_s/R_p)^2$.

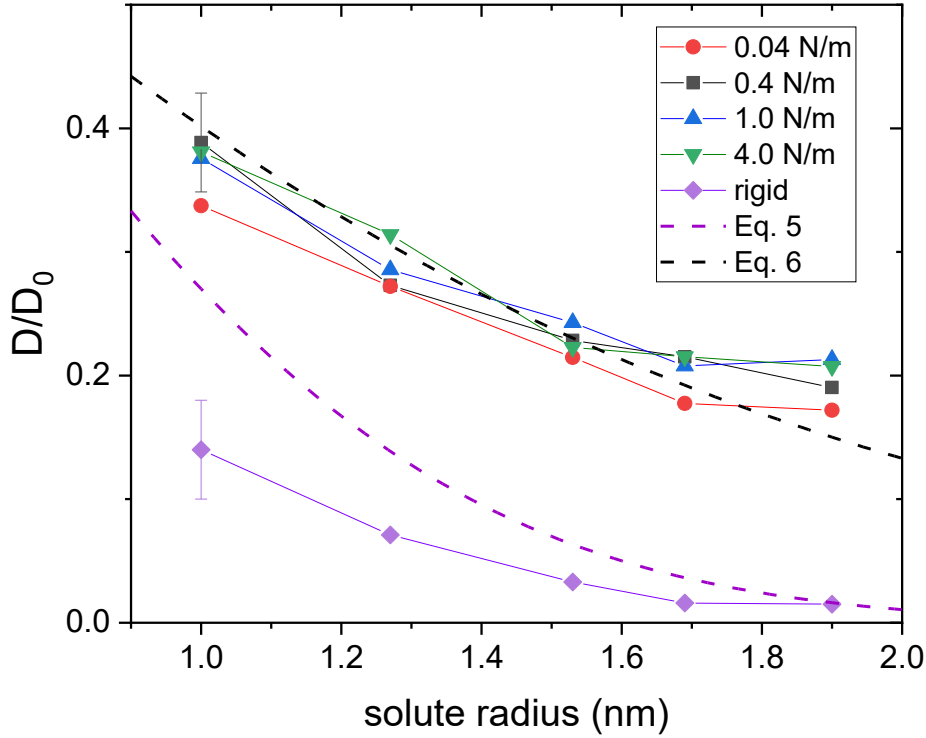


Figure 3. Relative diffusivity as a function of the solute radius for hydrogels with $N_{mu} = 25$ at $T = 293$ K, $\varphi = 0.08$, and different elastic constants: $k_e = 0.04$ (circles), 0.40 (squares), 1.0 (up triangles) and 4.0 (down triangles) N/m. The solute radius is 1.0 nm. The results for a rigid hydrogel (diamonds) and the prediction proposed by Johansson *et al.*¹⁰, Equation 5 (dashed magenta line) and Quesada-Pérez *et al.*⁴², Equation 6 (dashed black line), are also plotted for comparison.

This figure also confirms that the relative diffusivity in gels does not strongly depend on the elastic constant (at least, in the range of this parameter studied). It should be pointed out, however, that the effect of chain flexibility is larger for greater solutes. A similar conclusion was previously found comparing the predictions of Equation 6 and experimental diffusivities for different solutes in hydrogels based on PEGDA.⁴² In fact, Kamerlin and Elvingson concluded that diffusion in flexible networks is possible even for solute sizes well above the mean pore diameter.³⁶ The effect of the mesh size in flexible gels will be discussed in detail later. The prediction of Equation 5 is again plotted for comparison. Although the polymer fraction volume used in Figure 2 is outside the

validity range of Equation 5, it is interesting to observe that these theoretical predictions converge to the relative diffusivity obtained from simulations for rigid gels and greater solutes.

Effect of particle stiffness.

To begin this subsection, we should remember that, according to our model, the interaction between the solute particle and the monomers forming the hydrogel is purely steric (i.e., its origin is excluded volume). Here this interaction is modelled through the WCA potential, whose strength (ϵ_{WCA}) depends on the stiffness of the interacting particles. Thus, it is worth assessing the effect of this parameter on solute diffusion. Figure 4 shows the relative diffusivity as a function of the polymer volume fraction for two systems that only differ in the ϵ_{WCA} -value ($4.11 \cdot 10^{-21}$ and $4.11 \cdot 10^{-22}$ J, respectively). The rest of parameters are identical ($N_{mu} = 25$, $k_e = 0.4$ N/m, $R_s=1$ nm, $T = 293$ K). As can be easily concluded from this figure, diffusion is faster for soft solutes and/or monomeric units. This could be justified as follows. When ϵ_{WCA} decreases, particles may overlap to a greater degree. In other words, the effective excluded volume is smaller and this is equivalent to a reduction of the effective polymer volume fraction, which leads to an increase in diffusivity.

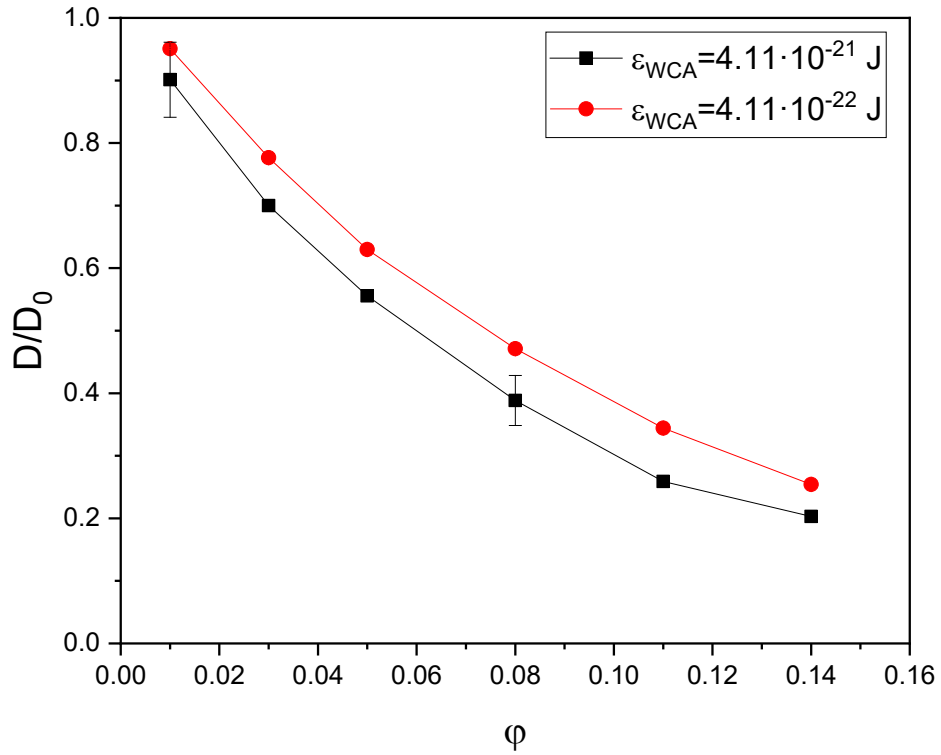


Figure 4. Relative diffusivity as a function of the polymer volume fraction for two hydrogels with different ϵ_{WCA} -values: $4.11 \cdot 10^{-21}$ (squares) and $4.11 \cdot 10^{-22}$ J (circles). The rest of parameters are $N_{mu} = 25$, $k_e = 0.4$ N/m, $R_s = 1$ nm, $T = 293$ K.

It is worth examining the case of larger solutes. Figure 5 displays the relative diffusivity as a function of the solute radius for $\phi = 0.08$ ($N_{mu} = 25$, $k_e = 0.4$ N/m, $T = 293$ K). By varying the size of the solute, the same conclusion is reached: diffusion is faster with decreasing ϵ_{WCA} .

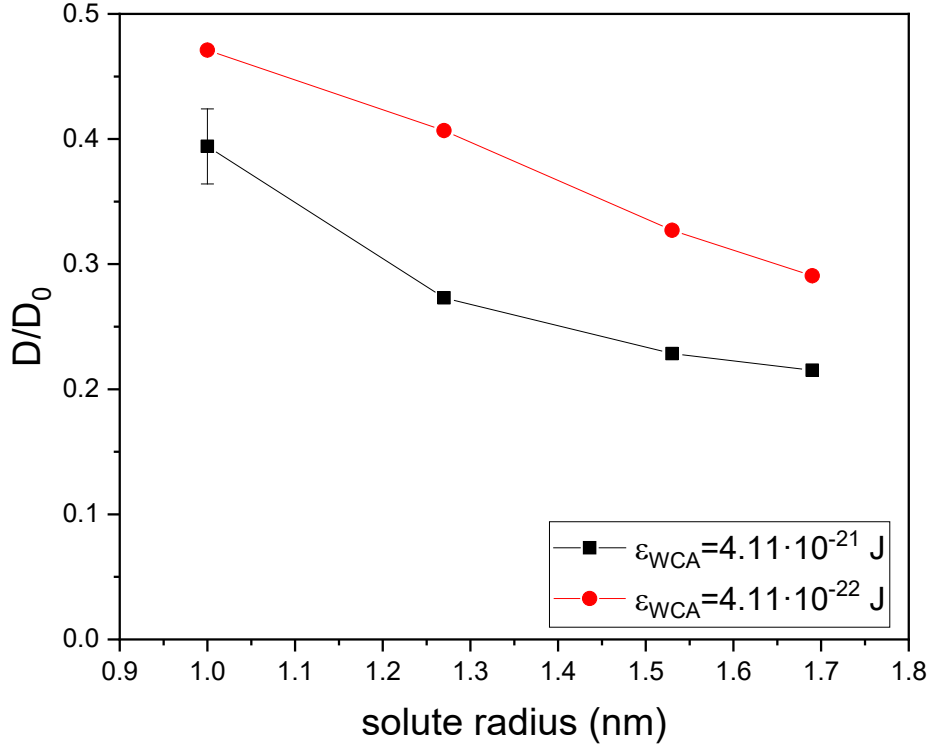


Figure 5. Relative diffusivity as a function of the solute radius for two hydrogels with different ϵ_{WCA} -values: $4.11 \cdot 10^{-21}$ (squares) and $4.11 \cdot 10^{-22}$ J (circles). The rest of parameters are $N_{mu} = 25$, $k_e = 0.4$ N/m, $\varphi = 0.08$, $T = 293$ K.

Effect of the degree of crosslinking.

We have also performed simulations of hydrogels with different degrees of crosslinking varying the number of monomeric units between two crosslinker molecules (N_{mu}). More specifically, we simulated hydrogels with $N_{mu} = 10$, 25 and 40 at different polymer volume fractions while the rest of parameters remained fixed ($k_e = 0.4$ N/m, $R_s=1$ nm, $T = 293$ K). The relative diffusivity is plotted as a function of φ in Figure 6.

As can be concluded, the effect of the degree of crosslinking on diffusion is negligible in the range of N_{mu} -values studied here. In relation to Figure 6, we should keep in mind that our simulations are performed in the canonical ensemble and the volume of the simulation cell is adjusted to the desired volume fraction. This allows us to easily simulate gels with different degrees of crosslinking but the same polymer volume fraction. In practice, this

is not so easy because these systems usually exert different osmotic pressures whereas this parameter remains fixed in many experiments. In other words, polymer volume fraction and degree of crosslinking are usually coupled in real hydrogels due to experimental conditions (constant osmotic pressure). Therefore, it is difficult to vary one of them without changing the other.

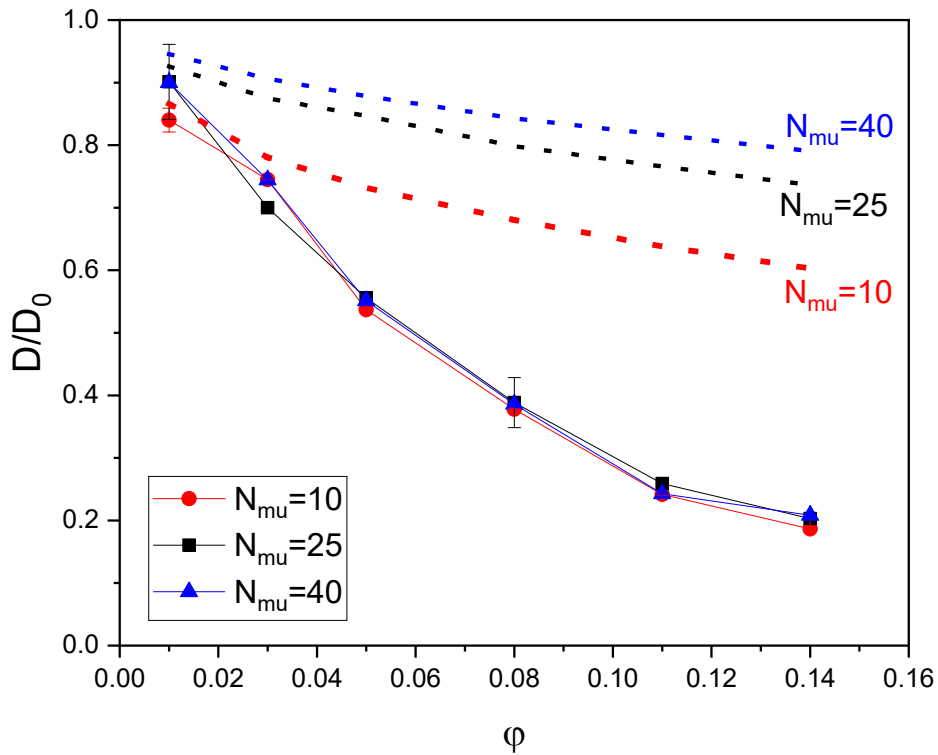


Figure 6. Relative diffusivity as a function of the polymer volume fraction obtained in simulations of gels with 10 (squares), 25 (circles) and 40 (up triangles) monomeric units per chain. The rest of parameter are $k_e = 0.4$ N/m, $R_s = 1$ nm, $T = 293$ K. The predictions of the obstruction model proposed by Amsden^{1,48} (dashed lines), Equation 7, are also plotted for comparison.

At this point, it is quite instructive to provide and analyze the mean distance between nodes (crosslinker molecules) of these gels. This parameter, which is usually known as mesh size (ξ), is plotted in Figure 7 for the three gels studied in Figure 6. The uncertainty of this parameter was estimated as the standard deviation of its fluctuations, which can be monitored during simulations. As can be seen, ξ is greater than the solute diameter (2 nm)

for gel with $N_{mu} = 25$ and 40. However, the mesh size is just a bit larger than the solute diameter for gels with $N_{mu} = 10$ at $\varphi > 0.1$. In spite of this, solute particles diffuse as fast as in gels with $N_{mu} = 40$. This suggests that the chain flexibility considerably facilitates the diffusion of particles whose diameter is close to the mesh size. Godec *et al.* and Kumar *et al.* came to similar conclusions for flexible gel-like structures.^{26,27} Godec and coworkers evaluated the time averaged mean squared displacement and the van-Hove cross-correlation function concluding that, when the size of solute particles is comparable to the mesh size, the particles still move in the gel but at a massively reduced diffusivity.²⁷ Kumar *et al.* computed the self-part of the van-Hove function (VHF) and showed that moderately sticky larger probes in a relatively flexible matrix stretch the network and have a finite but small probability to make large amplitude motion.²⁶ To shed light on the mechanism of diffusion in this case (diameter close to the mesh size), we have also computed the self-part of the VHF (see Supporting Information) for $N_{mu} = 10$ and $\varphi \geq 0.05$. This function reveals that, overall, the displacements corresponding to these cases are normally distributed. At large displacements, however, small deviations from the Gaussian distribution are found for $\varphi = 0.14$, particularly at long lag times. According to Kumar *et al.*,²⁶ such deviations suggest that the solute particle stretches the polymer network.

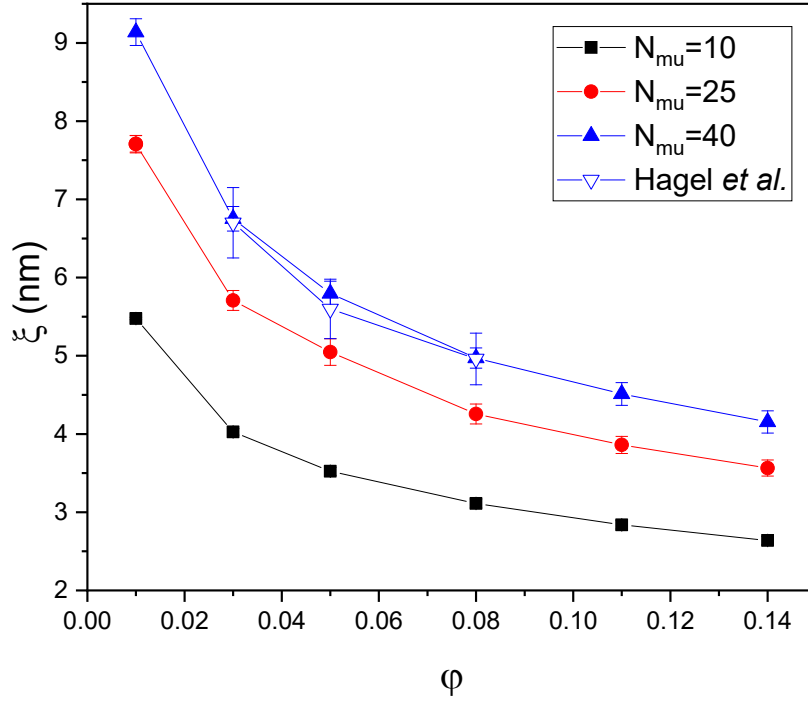


Figure 7. Mesh size as a function of the polymer volume fraction obtained in simulations of gels with 10 (squares), 25 (circles) and 40 (up triangles) monomeric units per chain. The error bars corresponding to 10 monomeric units per chain are smaller than the symbols. The mesh size for PEGDA hydrogels estimated by Hagel *et al.*⁴⁵ is also plotted (down triangles).

Jointly analyzed, Figures 6 and 7 also reveal that flexible gels with same volume fraction but different mesh sizes exhibit almost identical diffusion coefficients. In relation to this, it should be mentioned that Amsden derived an expression for the relative diffusivity of hydrogels composed of rigid polymer chains:^{1,48}

$$D/D_0 = \exp\left(-\pi \left(\frac{R_s + R_f}{\xi + 2R_f}\right)^2\right) \quad (7)$$

Here R_f is the fiber radius. As can be seen, this expression gives prominence to the mesh size, which explicitly appears instead of the polymer volume fraction. Amsden also suggested that this expression could be applied to hydrogels made of flexible chains and recently it was included in a multiscale model for solute diffusion in hydrogels.³

However, this expression dramatically fails as compared to our simulation results since it predicts different diffusivities for $N_{mu} = 10, 25$ and 40 . This is clearly illustrated in Figure 6, which also shows the predictions of Equation 7 calculated from the ξ -values obtained in simulation (Figure 7). It should be also mentioned that this obstruction theory considerably overestimates the diffusivity, particularly at high volume fractions. This result is surprising, since the theory was developed for rigid gels. Thus, one should expect diffusivities smaller than those obtained for flexible gels instead of significantly larger ones. Axpe *et al.* also concluded that this obstruction theory systematically tends to overestimate the diffusivity, except for very large solutes.³

Comparison with experimental data.

Recently, Majer and Southan have measured the diffusion coefficient of adenosine triphosphate (ATP) in twelve hydrogels based on poly(ethylene glycol) diacrylate with polymer volume fractions ranging from 0.06 to 0.30.⁴⁴ These researchers also tried to fit their data with three theories belonging to the three families commented in the introduction. According to their results, the hydrodynamic model proposed by Cukier is not able to capture the behavior found in their experiments. The obstruction model derived by Mackie and Meares succeeds in fitting the experimental data only if the polymer volume fraction is multiplied by a factor of 1.66. In the case of the free volume theory put forward by Lustig and Peppas, Majer and Southan first derived a phenomenological relationship between their estimates of mesh size and the polymer volume fraction and then they used the scale factor of the mentioned theory (Y) as fitting parameter. These authors obtained that $Y = 4.7$, but according to the free volume theory, this parameter should be of the order of 1. For the obstruction theory and the free volume theory, Majer and Southan employed fitting parameters whose values are not known a

priori and can probably change from case to case. Strictly speaking, these models can only fit data, not predict.

Thus, it would be quite interesting to find out if the coarse-grained model of polymer network employed here can really predict these experimental data. As mentioned previously, a key parameter of the model is the mean number of monomeric units per chain, which depends on the monomer-to-crosslinker ratio. Luckily, the molecular weight between crosslinks (M_c) can be estimated from data provided by Majer and Southan applying a modified version of the Flory-Rhener equation (see Equation 3 in Reference ⁴⁴). Then, $N_{mu} = M_c/M_{mu}$, where M_{mu} is the molecular weight of the monomeric unit of poly(ethylene glycol) chains ($-CH_2 - CH_2O -$). Table 1 shows the N_{mu} -values calculated for the twelve hydrogels studied by Majer and Southan (and presented in the same order). This table also shows the mean distance between crosslinks (mesh size) estimated by Majer and Southan.⁴⁴ As can be seen, there are three pairs of hydrogels with the same polymer volume fractions (0.06, 0.09 and 0.13, gels 7 and 11, 8 and 12, 5 and 9, respectively) but different values of N_{mu} and mesh size. Other parameters used in these simulations were $k_e = 0.4$ N/m, $R_s=0.633$ nm, $T = 298$ K, $\eta = 0.000891$ Pa·s and $\epsilon_{WCA} = 4.11 \cdot 10^{-21}$ J (the value of this parameter was used in previous works⁴⁹⁻⁵²). None of them was adjustable.

Table 1. Some parameters of the gels studied by Majer and Southan: polymer volume fraction (ϕ), molecular weight between crosslinks (M_c) estimated from the Flory-Rhener equation, number of monomers per chain employed in our simulations (N_{mu}) and mesh size (ξ) estimated by Majer and Southan.⁴⁴

Gel	Polymer volume fraction (ϕ)	Molecular weight between crosslinks (M_c , g/mol)	Number of monomers per chain (N_{mu})	Mesh size (ξ , nm)
1	0.1	242.7	6	2.6
2	0.2	157.2	4	1.6
3	0.3	105.0	2	1.1
4	0.07	917.4	21	6.0
5	0.13	606.6	14	3.9
6	0.16	584.5	13	3.4
7	0.06	1466.2	33	7.7
8	0.09	1300.0	30	6.0
9	0.13	992.9	23	5.0
10	0.03	3036.5	69	12.9
11	0.06	2331.9	53	8.9
12	0.09	1849.8	42	7.5

In Figure 8, the relative diffusivity measured by Majer and Southan is plotted as a function of the polymer volume fraction. Diffusivities obtained from simulations are also plotted for comparison. Overall, the agreement between experiment and simulation is quite good, particularly if we keep in mind that adjustable parameters were not employed in our simulations. Clear discrepancies between experiment and simulation are only observed for two polymer volume fractions (0.10 and 0.20). But the measured data corresponding to these ϕ -values also deviate from the trend line of the rest of experimental points. Consequently, we should not put too much emphasis on the previously mentioned

discrepancies between simulation and experiment. In any case, the agreement between simulation results (which do not consider hydrodynamic forces) and experimental data suggests that hydrodynamic interactions do not play a key role here. In Supporting Information, the reader can find preliminary simulations on the effect of hydrodynamic interactions on flexible gels.

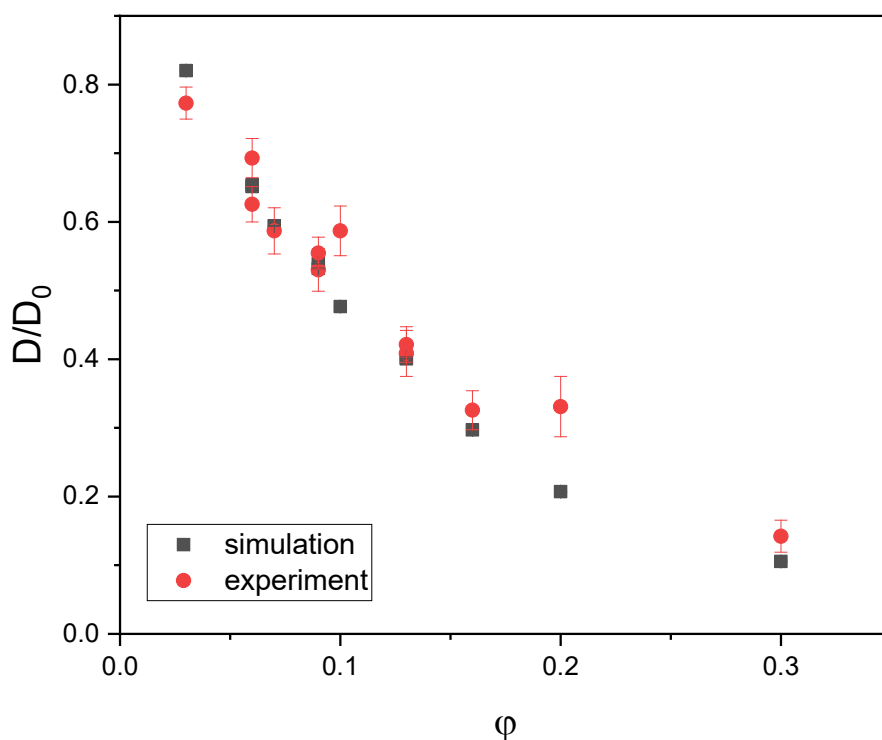


Figure 8. Relative diffusivity measured by Majer and Southan.⁴⁴ for ATP in PEGDA hydrogels (circles) and predicted by the model of flexible and crosslinked gel employed here (squares).

At this point, let us turn our attention to the diffusivities of the three pairs of points corresponding to the polymer volume fractions 0.06 (samples 7 and 11), 0.09 (samples 8 and 12) and 0.13 (samples 5 and 9). As can be concluded from Figure 8, Majer and Southan measured similar diffusion coefficients for each pair of hydrogels with the same ϕ -value despite the fact that these pairs differ in the number of monomeric units per chain

and in the mesh size. This behavior is perfectly captured by simulations, which also predict similar coefficients for such pairs.

Hagel *et al.* also studied solute diffusion in PEGDA hydrogels.⁴⁵ In this case, they measured the diffusion coefficient of monodisperse dextran particles with diameters ranging from 1.9 to 2.6 nm. These authors tried to fit their experimental data for different solute sizes with the Ogstons model using the fiber radius as adjustable parameter. The fits were acceptable but got worse with the polymer volume fraction. Different values of the fiber radius were obtained from the fits for series of data at different polymer volume fractions. More specifically, the fiber radius varied from 0.48 to 0.72 nm. These values are considerably greater than the monomer radius estimated for ethylene glycol (of the order of 0.3 nm).

It would be interesting to find out to what extent the model of flexible hydrogel employed here can predict the relative diffusivities reported by Hagel *et al.* without using adjustable parameters. Unfortunately, these authors did not provide information to straightforwardly compute M_c or M_{mu} . But the number of monomers per chain can be indirectly obtained from the estimates of mesh sizes that these researchers reported if such ξ -values are also plotted in Figure 7. As can be seen, these data agree quite well with those obtained from simulations for $N_{mu} = 40$. Consequently, we assume that the PEDGA chains synthesized by Hagel *et al.* are made of 40 monomers per chain (on average). The rest of parameters were $k_e = 0.4$ N/m, $T = 298$ K and $\eta = 0.000891$ Pa·s.

Figure 9 shows the relative diffusivity measured by Hagel *et al.* and those obtained from simulations as a function of the solute radius for two volume fractions (0.03 and 0.05). Since the polymer volume fraction and the solute radius are within the ranges simulated by Johansson and Löfroth ($\varphi \leq 0.05$ and $R_s \leq 3.0$ nm),¹⁰ the predictions of Equation 5 are also plotted as reference of rigid gels. As can be seen for $\varphi = 0.03$, the agreement

between simulation and experiment is acceptable considering that no adjustable parameters were used. In contrast, the prediction of Equation 5 clearly fails when the solute diameter increases. This reveals once more that the role played by the chain flexibility is important for large solute diameters and high φ -values. For $\varphi = 0.05$, the diffusivities predicted by simulations also deviates from the experimental values for large solutes diameters, although simulations again provide diffusivities much closer to the experimental values than Equation 5. Regarding these discrepancies between simulations and experiments, it should be mentioned that the model of network used here considers certain degree of disorder associated to fluctuations in the polymer chains. But this model could be improved by including some defects in the network, such as chains of different lengths, entanglements or loose chains. Such defects may be common in real gels, so it would be interesting to consider them in future works as some researchers have already done.^{40,41} In any case, the predictions based on these models would require the knowledge of structural parameters whose experimental determination can be complex, such as the mesh size and the connectivity. Recently it has been shown that the simultaneous measurement of the particle free energy and the particle diffusion coefficient helps to determine such parameters.⁵³

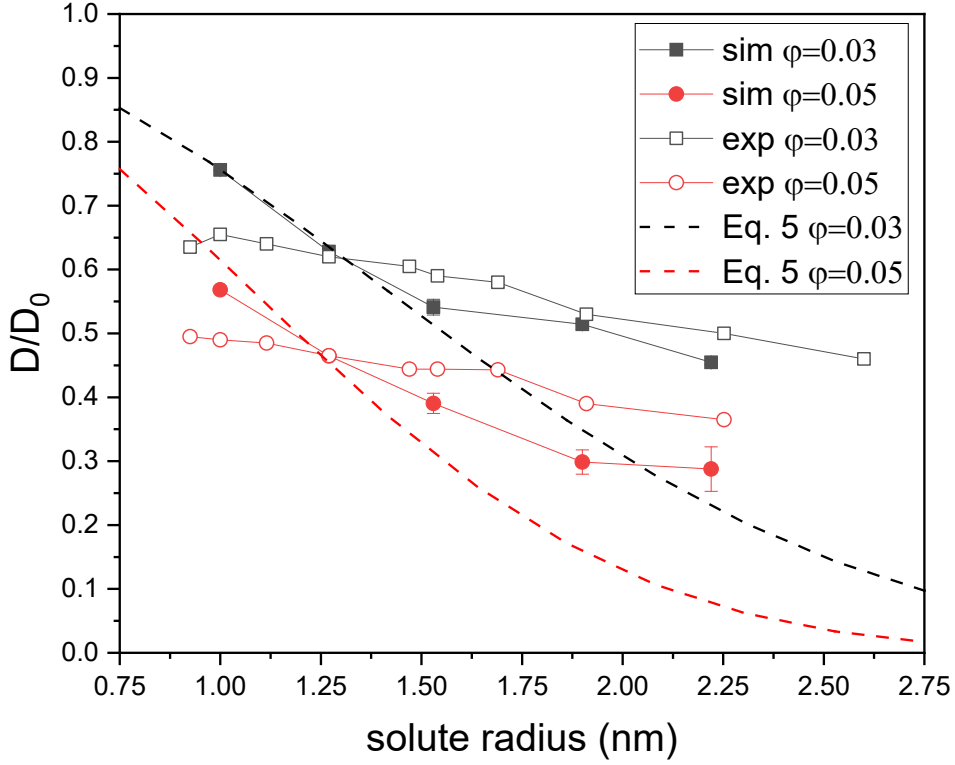


Figure 9. Relative diffusivity measured by Hagel *et al.*⁴⁵ in PEGDA hydrogels at $\varphi = 0.03$ (open squares) and $\varphi = 0.05$ (open circles) as a function of the solute radius. The results obtained from simulation at $\varphi = 0.03$ (solid squares) and $\varphi = 0.05$ (solid circles) and the prediction of Equation 5 at $\varphi = 0.03$ (black dashed line) and $\varphi = 0.05$ (red dashed line) are also plotted for comparison.

Anomalous diffusion

This work has focused on the longtime diffusive motion, whose MSD is described by Equation 4. It should be mentioned however, that the behavior of the MSD could be affected by the flexibility of the polymer chains at other time scales. In the limit of very short times, the perturbation of the polymeric network hardly affects the motion of the solute, which diffuses almost freely. Thus the MSD is also proportional to time (at least in the asymptotic limit), but the corresponding diffusion coefficient tends to D_0 instead of D . Consequently, there must be a transient regime between these two diffusive motions. In this intermediate regime, the MSD is usually proportional to t^n (with $n < 1$),

which is known as anomalous diffusion.⁵⁴⁻⁵⁶ We have computed the exponent of anomalous diffusion (n) for the gel with $N_{mu} = 25$ and $k_e = 0.4$ N/m at 293 K (and different φ -values) and a solute particle with $R_s=1$ nm following the method proposed by Netz *et al.*¹². According to these authors, $\log(\langle\Delta r^2\rangle/t)$ is plotted against $\log(t)$. The slope of the transient regime provides the value of $n - 1$. The n -values obtained through this procedure are plotted as a function of the polymer volume fraction in Figure 10. The exponent of anomalous diffusion was also computed for a rigid gel with the same N_{mu} -value and plotted for comparison. As can be concluded, n is much smaller for the rigid gel at moderate polymer volume fractions. What is more, this parameter almost drops to zero for the two φ -values in which the solute remains trapped in a void of the polymer network (see discussion of Figure 2). In other words, anomalous diffusion is much more pronounced in rigid gels. Similar results were found in the molecular dynamics simulations carried out by Samanta and Chakrabarti.³⁹ They varied the polymer volume fraction and the parameter characterizing the binding affinity between monomers and the tracer particle concluding that, in the presence of frozen polymers, the n -exponent becomes negligible.

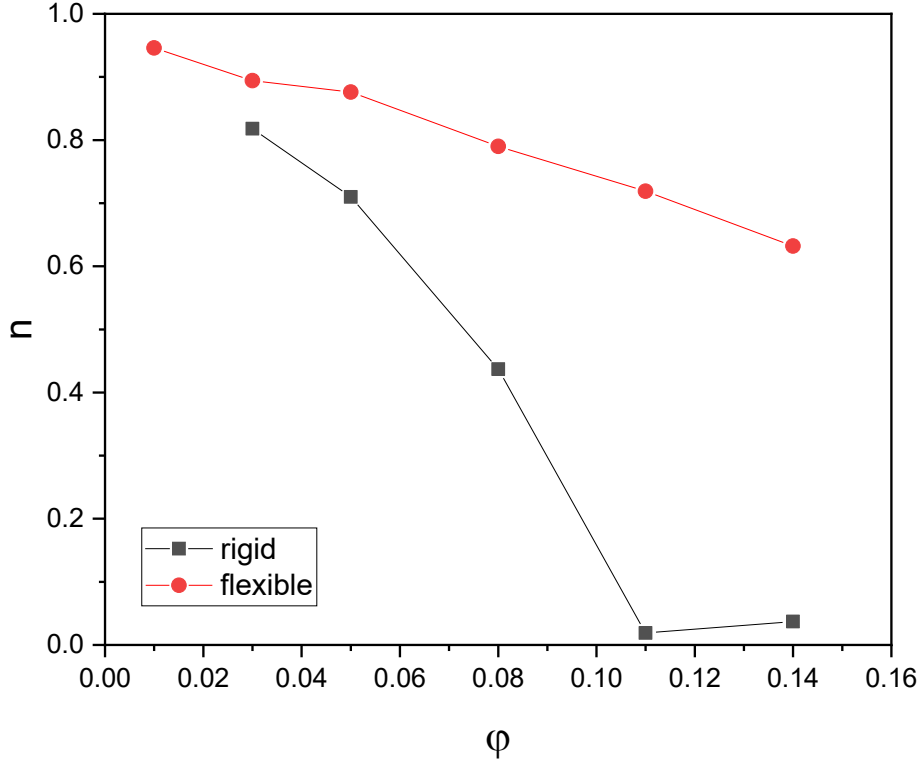


Figure 10. Exponent of anomalous diffusion as a function of the polymer volume fraction for hydrogels with $N_{mu} = 25$ and $k_e = 0.4$ N/m at 293 K and (solid circle). The solute radius is 1.0 nm. The results for a rigid hydrogel (solid square) are also plotted for comparison.

CONCLUSIONS

In this work, the long-time diffusion coefficients of spherical solute particles in different hydrogels have been computed through simulations within a coarse-grained model of gel made of flexible and crosslinked polymer chains. If the radius of the polymeric chains does not vary, diffusion is mostly controlled by two parameters: the polymer volume fraction and the solute radius. The stiffness of solute particles and/or monomeric units may have some influence on diffusion. However, our simulations reveal no significant effects of mesh size for solute diameters of just a few nanometers (as long as the polymer

volume fraction remains constant). In the range studied here, the elastic constant of the monomeric bonds does not have a significant influence on diffusion either.

In any case, the effect of chain flexibility becomes important when the polymer volume fraction and the solute radius increase. In fact, according to our simulations, solute particles might remain trapped inside rigid polymeric networks with polymer volume fractions of the order of 0.1 (and even lower) and moderately diffuse in flexible gels with the same φ . In addition, diffusion is possible when the mesh size is close to the solute diameter.

The results obtained from simulations reasonably agree with two different experiments without requiring adjustable parameters. In particular, the predictions of these simulations agree with the fact that hydrogels with the same polymer volume fraction but different degree of crosslinking and mesh size exhibit very similar diffusion coefficients. However, the quantitative agreement between simulations and experiments seems to get worse when the solute size increases.

Finally, we should keep in mind that the only solute/gel interaction considered in the coarse-grained model is the purely steric one. The presence of any other interaction between the solute and the gel in real systems could bring about deviations from the results reported here. For instance, electrostatic interactions are always present in charged systems and previous simulations performed within rigid gel-like systems suggest that they can play a fundamental role, particularly when solute and gel are oppositely charged.^{11,15,16,19,20,22,57} In this case, electrostatic forces might even bring about the immobilization of charged particles. Recently, some authors have also studied the diffusive behavior of tracer particles in the presence of sticky obstacles.^{26,39} This stickiness is responsible to a great extent for the subdiffusive motion.

Acknowledgements

The authors are grateful for funding from “Consejería de Economía, Conocimiento, Empresas y Universidad, Junta de Andalucía, Programa Operativo FEDER Andalucía 2014-2020”, Project PY20_00138. In addition, A. M.-M. thanks the financial support by the “Consejería de Conocimiento, Investigación y Universidad, Junta de Andalucía” and European Regional Development Fund (ERDF), Project SOMM17/6105/UGR. M. M. R.-T. also thanks the financial support by Ministerio de Ciencia e Innovación, Projects PGC2018-098770-B-I00 and PID2020-116615RA-I00.

Supporting Information: Examples of mean squared displacement, non-Gaussian parameter, van Hove function and effect of hydrodynamic forces.

References

- (1) Amsden, B. Solute Diffusion within Hydrogels. Mechanisms and Models. *Macromolecules* **1998**, *31* (23), 8382–8395. <https://doi.org/10.1021/ma980765f>.
- (2) Masaro, L.; Zhu, X. X. Physical Models of Diffusion for Polymer Solutions, Gels and Solids. *Prog. Polym. Sci.* **1999**, *24* (5), 731–775. [https://doi.org/10.1016/S0079-6700\(99\)00016-7](https://doi.org/10.1016/S0079-6700(99)00016-7).
- (3) Axpe, E.; Chan, D.; Offeddu, G. S.; Chang, Y.; Merida, D.; Hernandez, H. L.; Appel, E. A. A Multiscale Model for Solute Diffusion in Hydrogels. *Macromolecules* **2019**, *52* (18), 6889–6897. <https://doi.org/10.1021/acs.macromol.9b00753>.
- (4) Quesada-Pérez, M.; Martín-Molina, A. Solute Diffusion in Gels: Thirty Years of Simulations. *Adv. Colloid Interface Sci.* **2021**, 287. <https://doi.org/10.1016/j.cis.2020.102320>.

- (5) Casalini, T. Not Only in Silico Drug Discovery: Molecular Modeling towards in Silico Drug Delivery Formulations. *J. Control. Release* **2021**, *332*, 390–417. <https://doi.org/10.1016/j.jconrel.2021.03.005>.
- (6) Casalini, T.; Perale, G. From Microscale to Macroscale: Nine Orders of Magnitude for a Comprehensive Modeling of Hydrogels for Controlled Drug Delivery. *Gels*. 2019, p 28. <https://doi.org/10.3390/gels5020028>.
- (7) Ignacio, M.; Chubynsky, M. V; Slater, G. W. Interpreting the Weibull Fitting Parameters for Diffusion-Controlled Release Data. *Phys. A-STATISTICAL Mech. ITS Appl.* **2017**, *486*, 486–496. <https://doi.org/10.1016/j.physa.2017.05.033>.
- (8) Ignacio, M.; Slater, G. W. Using Fitting Functions to Estimate the Diffusion Coefficient of Drug Molecules in Diffusion-Controlled Release Systems. *Phys. A-STATISTICAL Mech. ITS Appl.* **2021**, *567*. <https://doi.org/10.1016/j.physa.2020.125681>.
- (9) Johansson, L.; Elvingson, C.; Löfroth, J. E. Diffusion and Interaction in Gels and Solutions. 3. Theoretical Results on the Obstruction Effect. *Macromolecules* **1991**, *24* (22), 6024–6029. <https://doi.org/10.1021/ma00022a019>.
- (10) Johansson, L.; Löfroth, J. Diffusion and Interaction in Gels and Solutions. 4. Hard Sphere Brownian Dynamics Simulations. *J. Chem. Phys.* **1993**, *98* (9), 7471–7479. <https://doi.org/10.1063/1.464686>.
- (11) Johansson, L.; Skantze, U.; Löfroth, J. E. Diffusion and Interaction in Gels and Solutions. 6. Charged Systems. *J. Phys. Chem.* **1993**, *97* (38), 9817–9824. <https://doi.org/10.1021/j100140a045>.
- (12) Netz, P. A.; Dorfmueller, T. Computer Simulation Studies of Anomalous Diffusion in Gels: Structural Properties and Probe-Size Dependence. *J. Chem. Phys.* **1995**, *103* (20), 9074–9082. <https://doi.org/10.1063/1.470018>.

- (13) Wedemeier, A.; Merlitz, H.; Wu, C. X.; Langowski, J. Modeling Diffusional Transport in the Interphase Cell Nucleus. *J. Chem. Phys.* **2007**, *127* (4).
<https://doi.org/10.1063/1.2753158>.
- (14) Netz, P. A.; Dorfmueller, T. Computer Simulation Studies of Diffusion in Gels: Model Structures. *J. Chem. Phys.* **1997**, *107* (21), 9221–9233.
<https://doi.org/10.1063/1.475214>.
- (15) Miyata, T.; Endo, A.; Ohmori, T.; Nakaiwa, M.; Kendo, M.; Kurumada, K.; Tanigaki, M. Brownian Dynamics Simulation Study of Self-Diffusion of a Charged Particle in Swollen Counter-Charged Hydrogel Modeled as Cubic Lattice. *J. Chem. Eng. JAPAN* **2002**, *35* (7), 640–648.
<https://doi.org/10.1252/jcej.35.640>.
- (16) Miyata, T. Brownian Dynamics Simulation of Self-Diffusion of Ionic Large Solute Molecule in Modeled Polyelectrolyte Gel. *J. Phys. Soc. Japan* **2012**, *81* (SUPPL. A), SA010. <https://doi.org/10.1143/JPSJS.81SA.SA010>.
- (17) Stylianopoulos, T.; Poh, M.-Z.; Insin, N.; Bawendi, M. G.; Fukumura, D.; Munn, L. L.; Jain, R. K. Diffusion of Particles in the Extracellular Matrix: The Effect of Repulsive Electrostatic Interactions. *Biophys. J.* **2010**, *99* (5), 1342–1349.
<https://doi.org/10.1016/j.bpj.2010.06.016>.
- (18) Stylianopoulos, T.; Diop-Frimpong, B.; Munn, L. L.; Jain, R. K. Diffusion Anisotropy in Collagen Gels and Tumors: The Effect of Fiber Network Orientation. *Biophys. J.* **2010**, *99* (10), 3119–3128.
<https://doi.org/10.1016/j.bpj.2010.08.065>.
- (19) Zhang, X.; Hansing, J.; Netz, R. R.; Derouchey, J. E. Particle Transport through Hydrogels Is Charge Asymmetric. *Biophys. J.* **2015**, *108* (3), 530–539.
<https://doi.org/10.1016/j.bpj.2014.12.009>.

- (20) Hansing, J.; Ciemer, C.; Kim, W. K.; Zhang, X.; DeRouchey, J. E.; Netz, R. R. Nanoparticle Filtering in Charged Hydrogels: Effects of Particle Size, Charge Asymmetry and Salt Concentration. *Eur. Phys. J. E* **2016**, *39* (5), 53. <https://doi.org/10.1140/epje/i2016-16053-2>.
- (21) Hansing, J.; Netz, R. R. Particle Trapping Mechanisms Are Different in Spatially Ordered and Disordered Interacting Gels. *Biophys. J.* **2018**, *114* (11), 2653–2664. <https://doi.org/10.1016/j.bpj.2018.04.041>.
- (22) Hansing, J.; Netz, R. R. Hydrodynamic Effects on Particle Diffusion in Polymeric Hydrogels with Steric and Electrostatic Particle-Gel Interactions. *Macromolecules* **2018**, *51* (19), 7608–7620. <https://doi.org/10.1021/acs.macromol.8b01494>.
- (23) Licinio, P.; Teixeira, A. V. Anomalous Diffusion of Ideal Polymer Networks. *Phys. Rev. E* **1997**, *56* (1, B), 631–634. <https://doi.org/10.1103/PhysRevE.56.631>.
- (24) Zhou, H.; Chen, S. B. Brownian Dynamics Simulation of Tracer Diffusion in a Cross-Linked Network. *Phys. Rev. E* **2009**, *79* (2). <https://doi.org/10.1103/PhysRevE.79.021801>.
- (25) Sandrin, D.; Wagner, D.; Sitta, C. E.; Thoma, R.; Felekyan, S.; Hermes, H. E.; Janiak, C.; De Sousa Amadeu, N.; Kühnemuth, R.; Löwen, H.; Egelhaaf, S. U.; Seidel, C. A. M. Diffusion of Macromolecules in a Polymer Hydrogel: From Microscopic to Macroscopic Scales. *Phys. Chem. Chem. Phys.* **2016**, *18* (18), 12860–12876. <https://doi.org/10.1039/c5cp07781h>.
- (26) Kumar, P.; Theeyancheri, L.; Chaki, S.; Chakrabarti, R. Transport of Probe Particles in a Polymer Network: Effects of Probe Size, Network Rigidity and Probe-Polymer Interaction. *Soft Matter* **2019**, *15* (44), 8992–9002. <https://doi.org/10.1039/c9sm01822k>.

- (27) Godec, A.; Bauer, M.; Metzler, R. Collective Dynamics Effect Transient Subdiffusion of Inert Tracers in Flexible Gel Networks. *New J. Phys.* **2014**, *16*, 092002. <https://doi.org/10.1088/1367-2630/16/9/092002>.
- (28) Schneider, S.; Linse, P. Monte Carlo Simulation of Defect-Free Cross-Linked Polyelectrolyte Gels. *J. Phys. Chem. B* **2003**, *107* (32), 8030–8040. <https://doi.org/10.1021/jp022336w>.
- (29) Mann, B. A.; Holm, C.; Kremer, K. Swelling of Polyelectrolyte Networks. *J. Chem. Phys.* **2005**, *122* (15), 154903. <https://doi.org/10.1063/1.1882275>.
- (30) Košovan, P.; Richter, T.; Holm, C. Molecular Simulations of Hydrogels. In *Intelligent Hydrogels*; Sadowski, G., Richtering, W., Eds.; Springer International Publishing, 2013; Vol. 140, pp 205–221. https://doi.org/10.1007/978-3-319-01683-2_16.
- (31) Yin, D.-W.; de la Cruz, M. O.; de Pablo, J. J. Swelling and Collapse of Polyelectrolyte Gels in Equilibrium with Monovalent and Divalent Electrolyte Solutions. *J. Chem. Phys.* **2009**, *131* (19). <https://doi.org/10.1063/1.3264950>.
- (32) Quesada-Pérez, M.; Adroher-Benítez, I.; Maroto-Centeno, J. A. Size-Exclusion Partitioning of Neutral Solutes in Crosslinked Polymer Networks: A Monte Carlo Simulation Study. *J. Chem. Phys.* **2014**, *140* (20), 204910. <https://doi.org/10.1063/1.4879215>.
- (33) Ahualli, S.; Martín-Molina, A.; Quesada-Pérez, M. Excluded Volume Effects on Ionic Partitioning in Gels and Microgels: A Simulation Study. *Phys. Chem. Chem. Phys.* **2014**, *16* (46), 25483–25491. <https://doi.org/10.1039/C4CP03314K>.
- (34) Pérez-Mas, L.; Martín-Molina, A.; Quesada-Pérez, M.; Moncho-Jordá, A. Maximizing the Absorption of Small Cosolutes inside Neutral Hydrogels: Steric

- Exclusion: Versus Hydrophobic Adhesion. *Phys. Chem. Chem. Phys.* **2018**, *20* (4). <https://doi.org/10.1039/c7cp07679g>.
- (35) Kim, W. K.; Moncho-Jordá, A.; Roa, R.; Kanduč, M.; Dzubiella, J. Cosolute Partitioning in Polymer Networks: Effects of Flexibility and Volume Transitions. *Macromolecules* **2017**, *50* (16), 6227–6237. <https://doi.org/10.1021/acs.macromol.7b01206>.
- (36) Kamerlin, N.; Elvingson, C. Tracer Diffusion in a Polymer Gel: Simulations of Static and Dynamic 3D Networks Using Spherical Boundary Conditions. *J. Phys. Condens. Matter* **2016**, *28* (47), 475101. <https://doi.org/10.1088/0953-8984/28/47/475101>.
- (37) Cho, H. W.; Kim, H.; Sung, B. J.; Kim, J. S. Tracer Diffusion in Tightly-Meshed Homogeneous Polymer Networks: A Brownian Dynamics Simulation Study. *Polymers (Basel)*. **2020**, *12* (9). <https://doi.org/10.3390/polym12092067>.
- (38) Milster, S.; Kim, W. K.; Kanduč, M.; Dzubiella, J. Tuning the Permeability of Regular Polymeric Networks by the Cross-Link Ratio. *J. Chem. Phys.* **2021**, *154* (15), 154902. <https://doi.org/10.1063/5.0045675>.
- (39) Samanta, N.; Chakrabarti, R. Tracer Diffusion in a Sea of Polymers with Binding Zones: Mobile vs. Frozen Traps. *Soft Matter* **2016**, *12* (41), 8554–8563. <https://doi.org/10.1039/c6sm01943a>.
- (40) Kim, W. K.; Chudoba, R.; Milster, S.; Roa, R.; Kanduč, M.; Dzubiella, J. Tuning the Selective Permeability of Polydisperse Polymer Networks. *Soft Matter* **2020**, *16* (35), 8144–8154. <https://doi.org/10.1039/D0SM01083A>.
- (41) Chen, Y.; Ma, R.; Qian, X.; Zhang, R.; Huang, X.; Xu, H.; Zhou, M.; Liu, J. Nanoparticle Mobility within Permanently Cross-Linked Polymer Networks. *Macromolecules* **2020**, *53* (11), 4172–4184.

- <https://doi.org/10.1021/acs.macromol.0c00334>.
- (42) Quesada-Pérez, M.; Maroto-Centeno, J. A.; Ramos-Tejada, M. del M.; Martín-Molina, A. Universal Description of Steric Hindrance in Flexible Polymer Gels. *Phys. Chem. Chem. Phys.* **2021**. <https://doi.org/10.1039/D1CP02113C>.
- (43) Tsuji, Y.; Li, X.; Shibayama, M. Evaluation of Mesh Size in Model Polymer Networks Consisting of Tetra-Arm and Linear Poly(Ethylene Glycol)S. *Gels* **2018**, *4* (2). <https://doi.org/10.3390/gels4020050>.
- (44) Majer, G.; Southan, A. Adenosine Triphosphate Diffusion through Poly(Ethylene Glycol) Diacrylate Hydrogels Can Be Tuned by Cross-Link Density as Measured by PFG-NMR. *J. Chem. Phys.* **2017**, *146* (22), 225101. <https://doi.org/10.1063/1.4984979>.
- (45) Hagel, V.; Haraszti, T.; Boehm, H. Diffusion and Interaction in PEG-DA Hydrogels. *Biointerphases* **2013**, *8* (1), 36. <https://doi.org/10.1186/1559-4106-8-36>.
- (46) Lin, C. C.; Anseth, K. S. PEG Hydrogels for the Controlled Release of Biomolecules in Regenerative Medicine. *Pharm. Res.* **2009**, *26* (3), 631–643. <https://doi.org/10.1007/s11095-008-9801-2>.
- (47) ERMAK, D. L. COMPUTER-SIMULATION OF CHARGED-PARTICLES IN SOLUTION .1. TECHNIQUE AND EQUILIBRIUM PROPERTIES. *J. Chem. Phys.* **1975**, *62* (10), 4189–4196. <https://doi.org/10.1063/1.430300>.
- (48) Amsden, B. An Obstruction-Scaling Model for Diffusion in Homogeneous Hydrogels. *Macromolecules* **1999**, *32* (3), 874–879. <https://doi.org/10.1021/ma980922a>.
- (49) Ramos-Tejada, M. D. M.; Quesada-Pérez, M. Coarse-Grained Simulations of Nanogel Composites: Electrostatic and Steric Effects. *Macromolecules* **2019**, *52*

- (6), 2223–2230. <https://doi.org/10.1021/acs.macromol.8b02657>.
- (50) Ahualli, S.; Martin-Molina, A.; Alberto Maroto-Centeno, J.; Quesada-Perez, M. Interaction between Ideal Neutral Nanogels: A Monte Carlo Simulation Study. *Macromolecules* **2017**, *50* (5), 2229–2238. <https://doi.org/10.1021/acs.macromol.6b02333>.
- (51) Adroher-Benítez, I.; Ahualli, S.; Martín-Molina, A.; Quesada-Pérez, M.; Moncho-Jordá, A. Role of Steric Interactions on the Ionic Permeation Inside Charged Microgels: Theory and Simulations. *Macromolecules* **2015**, *48* (13). <https://doi.org/10.1021/acs.macromol.5b00356>.
- (52) Perez-Mas, L.; Martin-Molina, A.; Quesada-Perez, M. Coarse-Grained Monte Carlo Simulations of Nanogel-Polyelectrolyte Complexes: Electrostatic Effects. *Soft Matter* **2020**, *16* (12), 3022–3028. <https://doi.org/10.1039/d0sm00173b>.
- (53) Wolde-kidan, A.; Herrmann, A.; Prause, A.; Gradzielski, M.; Haag, R.; Block, S.; Netz, R. R. Particle Diffusivity and Free-Energy Profiles in Hydrogels from Time-Resolved Penetration Data. *Biophysj* **2021**, *120* (3), 463–475. <https://doi.org/10.1016/j.bpj.2020.12.020>.
- (54) Metzler, R.; Jeon, J. H.; Cherstvy, A. G.; Barkai, E. Anomalous Diffusion Models and Their Properties: Non-Stationarity, Non-Ergodicity, and Ageing at the Centenary of Single Particle Tracking. *Phys. Chem. Chem. Phys.* **2014**, *16* (44), 24128–24164. <https://doi.org/10.1039/c4cp03465a>.
- (55) Ghosh, S. K.; Cherstvy, A. G.; Metzler, R. Non-Universal Tracer Diffusion in Crowded Media of Non-Inert Obstacles. *Phys. Chem. Chem. Phys.* **2015**, *17* (3), 1847–1858. <https://doi.org/10.1039/c4cp03599b>.
- (56) Cherstvy, A. G.; Thapa, S.; Wagner, C. E.; Metzler, R. Non-Gaussian, Non-Ergodic, and Non-Fickian Diffusion of Tracers in Mucin Hydrogels. *Soft Matter*

2019, *15* (12), 2526–2551. <https://doi.org/10.1039/c8sm02096e>.

- (57) Hansing, J.; Duke, J. R.; Fryman, E. B.; DeRouchey, J. E.; Netz, R. R. Particle Diffusion in Polymeric Hydrogels with Mixed Attractive and Repulsive Interactions. *Nano Lett.* **2018**, *18* (8), 5248–5256. <https://doi.org/10.1021/acs.nanolett.8b02218>.